

Tunable photoresponse of epitaxial graphene on SiC

Rujie Sun,¹ Ye Zhang,¹ Kang Li,² Chao Hui,¹ Ke He,² Xucun Ma,² and Feng Liu^{1,a)}

¹Department of Materials Science and Engineering, University of Utah, Salt Lake City, Utah 84112, USA

²Institute of Physics, Chinese Academy of Sciences, Beijing 100190, People's Republic of China

(Received 3 May 2013; accepted 16 June 2013; published online 1 July 2013)

We report photoresponse measurements from two comparable epitaxial graphene (EG) devices of different thicknesses (2-layer vs. \sim 10-layer EG) made on SiC substrates. An asymmetric metal contact scheme was used in a planar configuration to form a Ti/EG/Pd junction. By moving the laser illumination across the junction, we observed an increased photocurrent signal resulting from local enhancement of electric field near the metal/EG contact. A maximum photoresponsivity of 1.11 mA/W without bias was achieved at the Pd/EG contact in the 10-layer EG device. Photocurrent was also observed under AM 1.5 illumination. Our experiments demonstrate the high tunability of this EG photodetector by varying EG thickness, metal leads, channel length, and/or illumination area. © 2013 AIP Publishing LLC. [<http://dx.doi.org/10.1063/1.4812986>]

Graphene has attracted much recent attention because of its extraordinary electrical and optical properties that promise a wide range of device applications.^{1–5} For example, graphene photodetectors have been fabricated for high-speed optical communication,^{6,7} wide band optical detection,^{8–10} terahertz detection,^{11,12} and other applications.^{13–15} Graphene based photodetectors have been made using mechanically exfoliated graphene flakes,¹ CVD grown graphene,¹⁶ and epitaxial graphene (EG) on SiC substrates.^{17,18} Notably, EG on SiC can be fabricated as large-size, multi-layered devices, suitable for volume manufacturing due to good continuity, stability, and reproducibility.^{15,19} Additionally, the SiC substrate provides a convenient semi-insulating layer to support the EG device.¹⁹ Efficient and ultrafast photo detection⁶ has been achieved with an asymmetric metal contact configuration on exfoliated graphene flakes, which creates an asymmetric internal electric field between the source and drain contacts to direct the photocurrent.

In this letter, we report a very simple and direct methodology to fabricate EG photodetectors with an asymmetric metal contact configuration. Photocurrent was first observed by using a continuous-wave blue laser. The dependence of photocurrent on the laser-spot position was measured. An increased photocurrent signal was observed near the metal/EG contact, resulting from a locally enhanced electric field. A maximum photoresponsivity (PR) of 1.11 mA/W without bias was achieved at the Pd/EG contact in the 10-layer EG device. Photocurrent was also observed under AM 1.5 illumination using a solar simulator, showing practicality of EG for photo detecting devices.

Large-area EG samples were prepared on C-face 4H SiC substrates.^{20,21} For comparison, two different photodetectors were fabricated with EG film thicknesses of 2 and \sim 10 layers. The EG film quality was first characterized with atomic force microscopy (AFM) and Raman spectroscopy. Figure 1(a) shows a typical AFM scan of a 10-layer EG film, which has a local roughness of \sim 0.3 nm inside a 500 nm grain. Although the existence of grain boundaries in EG is

known to affect the carrier mobility,²² yielding lower device quantum efficiency, the overall photocurrent in our device was dominated by its large active area. Moreover, the two film thicknesses were verified by Raman spectra, as shown in Fig. 1(b).

Large-scale photodetectors were fabricated without involving any micro-scale fabrication technology. Fig. 1(c) shows the schematic drawing of the device configuration. Two metal electrodes (2×3.8 mm) were directly deposited onto a continuous EG film with a 2.4 mm wide separation. Asymmetric Ti and Pd metal electrodes of different work functions were used. A metal shadow mask was used to directly pattern electrodes in a Denton SJ20C electron beam evaporation system. 5 nm thick Ti and Pd were deposited on two ends and subsequently covered by a protective 20 nm thick Au layer to prevent oxidation.

Photocurrent for both the 2- and 10-layer EG devices was measured at ambient conditions. A 450 nm continuous wave laser system with adjustable power output and a visible light source from an AM 1.5 solar simulator were used as illumination sources. The energy of the laser (2.75 eV) was chosen to be below the band gap of 4H SiC (3.23 eV) to minimize the substrate contribution. As a control experiment, a benchmark device was made by depositing metal contacts directly onto a SiC substrate without EG; no significant photoresponse signal was detected from this device (see Fig. S1).²⁴ The laser beam was directed onto the sample surface with a 100 μ m diameter optical fiber while photocurrent measurement was performed by a Keithley 2420 I-V unit.

Because the metal contact layer is very thin, the laser is able to penetrate and reach the EG film, which adsorbs the most light. The difference in work function at the metal/EG interface forms an internal electric field, which leads to the generation and drift of free electrons upon photo excitation. The electric field drives the electrons from the high work function material to the low work function material. It is observed that photo electrons always flow from the metal lead to EG when laser or light is incident on either the Ti or Pd electrode. This indicates that EG has a work function lower than both Ti ($\Phi \sim 4.3$ eV) and Pd ($\Phi \sim 5.4$ eV), estimated to be in the range of 4.0 eV (see Fig. S2).²⁴

^{a)} Author to whom correspondence should be addressed. Electronic mail: fliu@eng.utah.edu

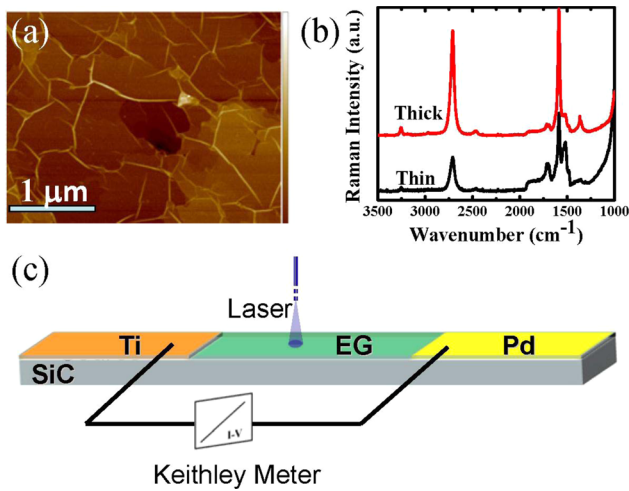


FIG. 1. (a) AFM scan of the 10-layer EG/SiC sample, Z-range = 15 nm; (b) Raman spectra of thin (~2-layer) and thick (~10-layer) EG films to analyze the number of layers on C-face SiC. (c) Schematics of the device with asymmetric Ti and Pd lead contacts, and a Keithley Source-Measure unit was used for I-V characterization.

To investigate the location dependence of photocurrent generation, the laser was scanned from the Ti side to the Pd side along the 2- and 10-layer EG devices. As shown in Fig. 2(a), the photocurrent signal was very strong when the laser directly illuminated the metal contact. When the laser illuminated the pure EG surface in between the two contacts, there was no electric field driving the photocurrent flow, and the signal was negligible. When the laser was incident at or near the Ti/EG or Pd/EG boundary, there was a local signal enhancement shown by a peak in the photocurrent curve. This can be explained by the local electrical field enhancement at the metal/EG boundary: in addition to the vertical field across the planar metal/EG interface, there exists also a

lateral field across the line boundary.²³ Overall, the thick EG generated more photocurrent because of its higher light absorption compared to the thin EG.

To investigate the relationship between the photo-generated current and light intensity, the I-V curves under different laser power illuminations were measured. A bias voltage in the range of ± 1 mV was applied between the source and drain contacts. Figure 2(b) shows the typical I-V curves of the thin 2-layer EG device illuminated by five different laser powers (0, 89, 201, 293, and 374 mW) on the Pd electrode side. The linear I-V curve shifts upward with increasing incident light intensity. The interceptions on the y-axis, i.e., the zero-bias photocurrents, illustrate that the amount of charge carriers generated by the laser illumination increased monotonically with increasing laser power.

To quantify the relationship between the photo-generated current and light intensity, the photocurrent, extracted from Fig. 2(b), was plotted as a function of laser power. The photocurrent generated by both devices increased linearly up to the maximum laser power used, regardless of which electrode was illuminated (see Fig. 2(c)). Also, a larger photocurrent was generated at the side of the Pd/EG junction compared to the side of the Ti/EG junction, as shown in the inset of Fig. 2(c). This could be caused by the larger difference in work function at the Pd/EG interface compared to the Ti/EG interface, leading to a larger internal field at the Pd/EG junction (or larger band bending of EG as shown in Fig. S2).²⁴ A linear fit of the photocurrent data in Fig. 2(c) gives constant PR of EG on SiC over a wide range of laser power. The maximum photoresponsivities without bias measured on the side of Pd/EG junction for the thick and thin EG devices are 1.11 and 0.88 mA/W, respectively.

The linear photoresponse to laser power observed in our EG devices is quite different from those made of

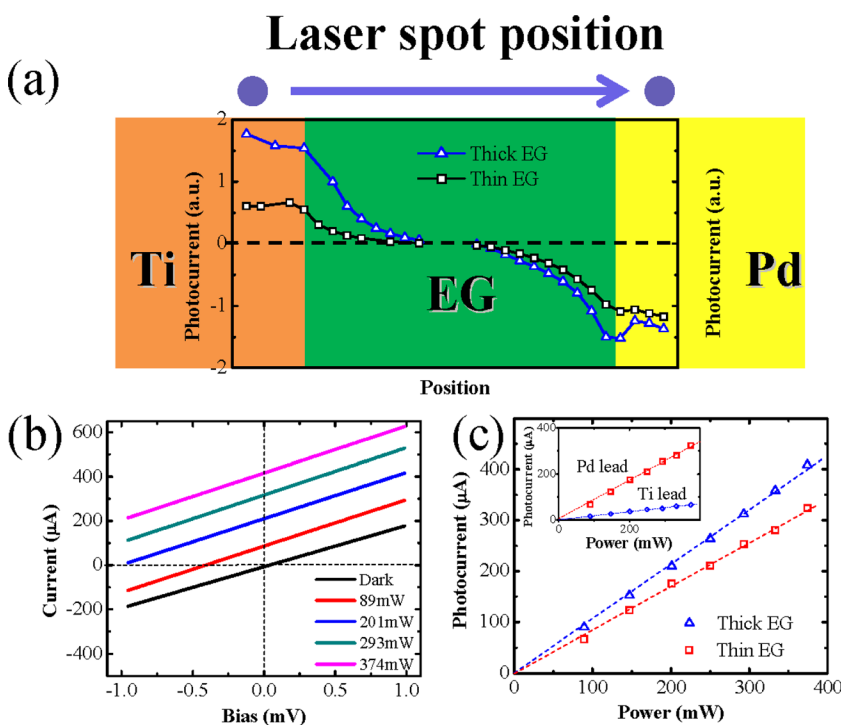


FIG. 2. Photoresponse of the Ti/EG/Pd device. (a) Photocurrent (arbitrary unit) of the thin and thick Ti/EG/Pd devices in response to laser illumination at different locations. (b) I-V curves of thick EG device under different laser illumination power. Laser spot was located on the Pd/EG junction; (c) photocurrent measured as a function of laser power at the Pd/EG junction from both the thin and thick EG devices. Inset shows the photocurrent measured from the thin EG device at the Pd/EG vs. Ti/EG junction.

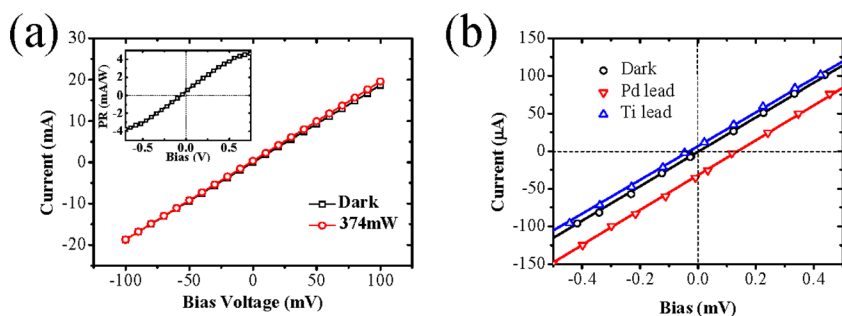


FIG. 3. (a) Current (I) as a function of source–drain bias (V) with and without light illumination at 450 nm wavelength. The inset shows the measured external PR as a function of the bias voltage. The I – V curves in open circle (red) and square (black) represent with and without illumination, respectively. (b) I – V curves of thick EG device under AM 1.5 illumination.

micron-size graphene flakes, whose photocurrent displays a saturation when the incident laser power is too high (see Fig. S3).^{6,24} In contrast, our EG devices have a wide range of linear photoresponse without saturation. We attribute this distinct advantage to their long channel length. Furthermore, our thick 10-layer device generates higher photocurrent than the thin 2-layer device, affording the opportunity to tune the device performance by varying the EG thickness in addition to varying device size (channel length and illumination area).

We also performed experiments to measure the photoconductivity of the devices by illuminating the Pd/EG junction while using a range of much larger bias voltages. Figure 3(a) shows the results obtained from the thin EG sample. With or without illumination, the device I – V curves show different characteristics, indicating a slight change of the photo induced conductivity from 0.187 to 0.192 Ω^{-1} . The inset of Fig. 3(a) shows the photoresponsivity initially increasing as a function of bias voltage, then saturating at high bias.¹⁹ A maximum photoresponsivity of ~ 4.5 mA/W was achieved with a bias of ~ 0.7 V.

The high PR (~ 1 mA/W) of our large-area EG devices indicated that a detectable signal could be obtained from ambient light illumination without using a laser source. To confirm this, we used a solar simulator with AM 1.5 visible light and a power density of ~ 100 mW/cm², which was much smaller than the laser source (190 000 mW/cm² for 0.5 mm spot size at maximum laser power). Figure 3(b) shows an observable photoresponse to the AM 1.5 light. The zero-bias PR was 4.08 mA/W at the active absorption area (2×3.8 mm) of the Pd/EG junction, significantly higher compared to our laser test at zero bias. We believe this is mainly due to photon absorption of a wide range of wavelengths, instead of a single wavelength. Also, a larger photocurrent signal is observed on the Pd/EG junction compared to the Ti/EG junction, in agreement with the laser testing results.

In summary, we demonstrated high photoresponse of large-area EG/SiC devices with asymmetric metal contacts. Photocurrent was generated from the internal electric field at the metal/EG junctions due to work function difference. High photoresponsivity was achieved with both coherent and incoherent light sources—laser and 1.5 AM solar simulator, respectively. The device performance is shown to be highly

tunable by varying metal leads, EG layer thickness, channel length, and/or illumination area.

This work was supported by Solan, LLC. We also thank Jason Merrell for proof reading the manuscript.

- ¹K. S. Novoselov, A. K. Geim, S. V. Morozov, D. Jiang, Y. Zhang, S. V. Dubonos, I. V. Grigorieva, and A. A. Firsov, *Science* **306**, 666 (2004).
- ²Y. Zhang, Y.-W. Tan, H. Stormer, and P. Kim, *Nature* **438**, 201 (2005).
- ³P. Avouris, Z. Chen, and V. Perebeinos, *Nat. Nanotechnol.* **2**, 605 (2007).
- ⁴R. Nair, P. Blake, A. Grigorenko, K. Novoselov, T. Booth, T. Stauber, N. Peres, and A. Geim, *Science* **320**, 1308 (2008).
- ⁵F. Wang, Y. Zhang, C. Tian, C. Girit, A. Zettl, M. Crommie, and Y. Shen, *Science* **320**, 206 (2008).
- ⁶T. Mueller, F. Xia, and P. Avouris, *Nature Photon.* **4**, 297 (2010).
- ⁷M. Liu, X. Yin, E. Ulin-Avila, B. Geng, T. Zentgraf, L. Ju, F. Wang, and X. Zhang, *Nature* **474**, 64 (2011).
- ⁸P. Blake, E. W. Hill, A. H. C. Neto, K. S. Novoselov, D. Jiang, R. Yang, T. J. Booth, and A. K. Geim, *Appl. Phys. Lett.* **91**, 063124 (2007).
- ⁹F. Xia, T. Mueller, Y.-M. Lin, A. Valdes-Garcia, and P. Avouris, *Nat. Nanotechnol.* **4**, 839 (2009).
- ¹⁰Y. Liu, R. Cheng, L. Liao, H. Zhou, J. Bai, G. Liu, L. Liu, Y. Huang, and X. Duan, *Nat. Commun.* **2**, 579 (2011).
- ¹¹L. Prechtel, L. Song, D. Schuh, P. Ajayan, W. Wegscheider, and A. W. Holleitner, *Nat. Commun.* **3**, 646 (2012).
- ¹²F. Xia, D. B. Farmer, Y.-M. Lin, and P. Avouris, *Nano Lett.* **10**, 715 (2010).
- ¹³F. Bonaccorso, Z. Sun, T. Hasan, and A. C. Ferrari, *Nat. Photonics* **4**, 611 (2010).
- ¹⁴B. Chitara, L. S. Panchakarla, S. B. Krupanidhi, and C. N. R. Rao, *Adv. Mater.* **23**, 5419 (2011).
- ¹⁵R. S. Singh, V. Nalla, W. Chen, A. T. S. Wee, and W. Ji, *ACS Nano* **5**, 5969 (2011).
- ¹⁶A. Reina, X. Jia, J. Ho, D. Nezich, H. Son, V. Bulovic, M. Dresselhaus, and J. Kong, *Nano Lett.* **9**, 30 (2009).
- ¹⁷W. A. de Heer, C. Berger, X. Wu, P. N. First, E. H. Conrad, X. Li, T. Li, M. Sprinkle, J. Hass, M. L. Sadowski *et al.*, *Solid State Commun.* **143**, 92 (2007).
- ¹⁸C. Berger, Z. Song, X. Li, X. Wu, N. Brown, C. Naud, D. Mayou, T. Li, J. Hass, A. N. Marchenkov *et al.*, *Science* **312**, 1191 (2006).
- ¹⁹R. S. Singh, V. Nalla, W. Chen, W. Ji, and A. T. S. Wee, *Appl. Phys. Lett.* **100**, 093116 (2012).
- ²⁰J. Hass, R. Feng, T. Li, X. Li, Z. Zong, W. A. de Heer, P. N. First, E. H. Conrad, C. A. Jeffrey, and C. Berger, *Appl. Phys. Lett.* **89**, 143106 (2006).
- ²¹F. Varchon, R. Feng, J. Hass, X. Li, B. Ngoc Nguyen, C. Naud, P. Mallet, J.-Y. Veullen, C. Berger, E. H. Conrad, and L. Magaud, *Phys. Rev. Lett.* **99**, 126805 (2007).
- ²²H. Song, S. Li, H. Miyazaki, S. Sato, K. Hayashi, A. Yamada, N. Yokoyama, and K. Tsukagoshi, *Sci. Rep.* **2**, 337 (2012).
- ²³F. Xia, T. Mueller, R. Golizadeh-Mojarad, M. Freitag, Y.-M. Lin, J. Tsang, V. Perebeinos, and P. Avouris, *Nano Lett.* **9**, 1039 (2009).
- ²⁴See supplementary material at <http://dx.doi.org/10.1063/1.4812986> for the photoresponse of a control SiC device, device band diagram, and the photoresponse of a few-layer graphene flake device.